

# Finite-Temperature Transition in the Spin-Dimer Antiferromagnet $\text{BaCuSi}_2\text{O}_6$

YOSHITOMO KAMIYA, NAOKI KAWASHIMA and CRISTIAN D. BATISTA<sup>1</sup>

*Institute for Solid State Physics, University of Tokyo, Kashiwa, Chiba 227-8581, Japan*

<sup>1</sup>*Theoretical Division, Los Alamos National Laboratory, Los Alamos, New Mexico 87545, USA*

We consider a classical XY-like Hamiltonian on a body-centered tetragonal lattice, focusing on the role of interlayer frustration. A three-dimensional (3D) ordered phase is realized via thermal fluctuations, breaking the mirror-image reflection symmetry in addition to the XY symmetry. A heuristic field-theoretical model of the transition has a decoupled fixed point in the 3D XY universality, and our Monte Carlo simulation suggests that there is such a temperature region where long-wavelength fluctuations can be described by this fixed point. However, it is shown using scaling arguments that the decoupled fixed point is unstable against a fluctuation-induced biquadratic interaction, indicating that a crossover to nontrivial critical phenomena with different exponents appears as one approaches the critical point beyond the transient temperature region. This new scenario clearly contradicts the previous notion of the 3D XY universality.

KEYWORDS: interlayer frustration; finite-temperature phase transition; order by disorder;  $Z_2$  symmetry breaking;  $\text{BaCuSi}_2\text{O}_6$

## 1. Introduction

Field-induced critical phenomena of gapped spin-dimer antiferromagnets have drawn much attention. Such antiferromagnets typically consist of strongly coupled spin-1/2 dimers, and are essentially in singlet states in zero field. Elementary excitations in the gapped phase under external magnetic fields are  $S_z = 1$  triplet excitations, sometimes called “triplons,” for which a magnetic field acts as a chemical potential. They undergo Bose-Einstein condensation (BEC) when their density is appropriately tuned.<sup>1)</sup>

$\text{BaCuSi}_2\text{O}_6$  is one of such spin-dimer compounds,<sup>2-14)</sup> with characteristic frustration in interlayer interactions. Spin dimers in this compound align on the body-centered tetragonal (BCT) lattice (Fig. 1). Owing to the lattice geometry, loops that include interlayer hoppings are frustrated, which leads to cancellation among interlayer interactions. An interesting behavior related to this interlayer frustration has been reported.<sup>15)</sup> The phase boundary around the quantum critical point is described by the power law  $T_c(H) \propto (H - H_c)^\phi$  with an anomalous exponent  $\phi = 1$ .<sup>2)</sup> Since mean-field treatment yields  $\phi = 2/d$ , the exponent is regarded as a characteristic of two-dimensional (2D) systems, and in this sense the phenomenon is called “dimensional reduction.” We refer to several recent papers for further details on this

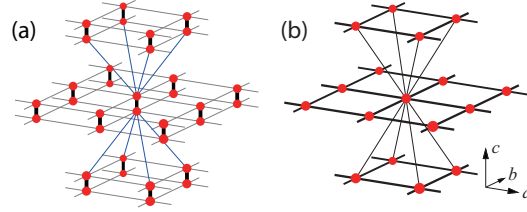


Fig. 1. (Color online) (a) Localized spin degrees of freedom in BaCuSi<sub>2</sub>O<sub>6</sub>. (b) BCT lattice. For clarity, interlayer bonds are drawn partially.

subject.<sup>2,10–14</sup>)

Our main interest in this paper is to study the critical properties at the finite temperature transition in BaCuSi<sub>2</sub>O<sub>6</sub>. Owing to the broken U(1) symmetry of the ordered state and a few experimental observations such as the  $\lambda$ -peak of specific heat,<sup>6</sup>) it has been presumed so far that the transition is in the three-dimensional (3D) XY universality class. However, as we will argue in this paper, the additional  $Z_2$  symmetry breaking that characterizes the ordered phase in the BCT lattice makes the XY fixed point unstable.<sup>10–13</sup>) The 3D XY-type order takes place in two subsystems or sublattices, namely, the even- and odd-numbered layers. The reason for this is that a  $Z_2$  mirror-image reflection symmetry of the BCT lattice precludes any bilinear effective coupling between layers on different sublattices. Although this  $Z_2$  symmetry allows biquadratic interlayer couplings making the order “collinear,” whether the XY antiferromagnetic (AF) moments of the sublattices are parallel or antiparallel remains undetermined, and one of them is selected via spontaneous  $Z_2$  symmetry breaking. The structure of this symmetry breaking is clearly different from that for the standard XY ordering, and our final goal is to understand the effect of the additional  $Z_2$  symmetry breaking on the universality class of the transition. For this purpose, we will study a classical spin model that will be introduced in the next section. A Hamiltonian for classical spins is adequate for describing the critical behavior near the critical temperature because the relevant (largest) fluctuations are classical: fluctuations in the imaginary time direction become negligible because they are confined to a finite size  $\beta = 1/T$ . We will also present numerical simulation results that elucidate the above-mentioned symmetry-breaking structure.

## 2. Model

The low-energy subspace generated by the  $S_z = 1$  triplet and singlet well approximates the spin-dimer systems in an applied magnetic field.<sup>1,16</sup>) The corresponding effective Hamiltonian is the XXZ model for  $S = 1/2$  pseudo-spins that represent the two states of each dimer:  $S^z = 1/2$  for the triplet and  $S^z = -1/2$  for the singlet. Since the the thermodynamic phase transition is driven by classical (or thermal) fluctuations, we can replace  $S = 1/2$  pseudo-spins with classical spins, in order to study the critical phenomena near the finite-temperature

transition:

$$\mathcal{H}_{cl} = J_{\parallel} \sum_{n, \langle \mathbf{r}, \mathbf{r}' \rangle} \mathbf{S}_{n, \mathbf{r}} \cdot \mathbf{S}_{n, \mathbf{r}'} + J_{\perp} \sum_{n, \mathbf{r}, \delta \mathbf{r}} \mathbf{S}_{n, \mathbf{r}} \cdot \mathbf{S}_{n+1, \mathbf{r} + \delta \mathbf{r}} - H \sum_{n, \mathbf{r}} S_{n, \mathbf{r}}^z, \quad (1)$$

where  $\mathbf{S}_{n, \mathbf{r}}$  is a three-component classical spin, located at a site  $\mathbf{r}$  in the  $n$ -th layer on the BCT lattice ( $\mathbf{r}$  refers to a two-component vector),  $\langle \mathbf{r}, \mathbf{r}' \rangle$  are nearest-neighbor pairs on a given layer, and  $\delta \mathbf{r} = (\pm a/2, \pm a/2)$  are interlayer displacement vectors (hereafter, we take  $a = 1$ ).  $J_{\parallel}$  ( $J_{\perp}$ ) is the AF intralayer (interlayer) interaction. Throughout the paper, we consider the case  $J_{\parallel} > J_{\perp} > 0$ , whose inequality sign is the same as that in the relation between the magnitudes of interdimer exchanges in  $\text{BaCuSi}_2\text{O}_6$ . The finite magnetic field  $H$  breaks  $O(3)$  spin symmetry down to  $O(2)$  symmetry, and thus the spins we treat are XY-like. This justifies the neglect of the easy-plane-type spin-anisotropy that exists in the effective XXZ model mentioned above. Although the two-component spins would serve the present purpose just as well as the three-component spins, we use the latter for technical reasons.

First, we will discuss the basic properties of  $\mathcal{H}_{cl}$ . The energy is minimized when the spins form a canted AF order in each layer. The ground-state configuration is given by

$$\mathbf{S}_{n, \mathbf{r}} = (\sin \Theta \cos \Phi_n e^{i\mathbf{Q} \cdot (\mathbf{r} - \mathbf{r}_0^{(n)})}, \sin \Theta \sin \Phi_n e^{i\mathbf{Q} \cdot (\mathbf{r} - \mathbf{r}_0^{(n)})}, \cos \Theta), \quad (2)$$

with  $\cos \Theta = H / [8(J_{\parallel} + J_{\perp})]$ ,  $\mathbf{Q} = (\pi, \pi)$ , and  $\mathbf{r}_0^{(n)} \equiv (\frac{1}{2}, \frac{1}{2}) \delta_{(-1)^n, 1}$ . We define  $\mathbf{M}_{XY}^{(n)} \equiv (\cos \Phi_n, \sin \Phi_n)$  to represent the XY AF moment of the  $n$ -th layer, and in what follows we use the term ‘‘AF moment’’ to refer to this quantity unless otherwise specified. Interlayer mean-field interactions cancel out in the ground state because of a combination of the intralayer AF order and the geometry of the BCT lattice. This means that the AF moments of one layer can be rotated without changing ground-state energy. Thus, the system may be viewed as a set of independent 2D layers at  $T = 0$ .

This apparent 2D character is lifted by thermal fluctuations. We will show that these fluctuations select a state qualitatively analogous to the ordered phase of the original quantum system. One of the simplest ways to see how this ‘‘order by disorder’’<sup>17,18)</sup> takes place is to use spin-wave approximation and evaluate free energy as a function of the ground-state configuration  $\{\Phi_n\}$ . Let  $\theta_{n, \mathbf{r}}$  and  $\phi_{n, \mathbf{r}}$  represent small fluctuations around a given ground-state configuration. Expanding the Hamiltonian to the second order in these variables, we rewrite it in the form  $\mathcal{H}_{cl} \approx \mathcal{H}_{sw}(\Theta, \{\Phi_n\}; \{\theta_{n, \mathbf{r}}\}, \{\phi_{n, \mathbf{r}}\}) = \mathcal{H}_{2D} + gV$  with  $g \equiv J_{\perp}/J_{\parallel}$ . Here,

$$\mathcal{H}_{2D} = \frac{1}{2} \sum_{n, \mathbf{q}} (\omega_{\theta}(\mathbf{q}) \theta_{n, \mathbf{q}} \theta_{n, -\mathbf{q}} + \omega_{\phi}(\mathbf{q}) \phi_{n, \mathbf{q}} \phi_{n, -\mathbf{q}}) \quad (3)$$

and

$$V = \sum_{n, \mathbf{q}} \left[ \gamma_{\theta\theta}^{(n)}(\mathbf{q}) \theta_{n, \mathbf{q}} \theta_{n+1, -\mathbf{q}} + \gamma_{\phi\phi}^{(n)}(\mathbf{q}) \phi_{n, \mathbf{q}} \phi_{n+1, -\mathbf{q}} + \gamma_{\theta\phi}^{(n)}(\mathbf{q}) (\theta_{n, \mathbf{q}} \phi_{n+1, -\mathbf{q}} - \theta_{n+1, -\mathbf{q}} \phi_{n, \mathbf{q}}) \right], \quad (4)$$

where  $\theta_{n, \mathbf{q}} = (L^2)^{-1/2} \sum_{\mathbf{r}} \theta_{n, \mathbf{r}} e^{-i\mathbf{q} \cdot \mathbf{r}}$  and  $\phi_{n, \mathbf{q}} = (L^2)^{-1/2} \sum_{\mathbf{r}} \phi_{n, \mathbf{r}} e^{-i\mathbf{q} \cdot \mathbf{r}}$  with  $L^2$  being the

number of sites in each layer. The coefficients in  $\mathcal{H}_{2D}$  are written as

$$\omega_\theta(\mathbf{q}) = 2J_\parallel [2 + (1 - 2\cos^2\Theta)(\cos q_x + \cos q_y)] \quad (5)$$

$$\omega_\phi(\mathbf{q}) = 2J_\parallel \sin^2\Theta (2 - \cos q_x - \cos q_y), \quad (6)$$

and those in  $V$  are written as

$$\gamma_{\theta\theta}^{(n)}(\mathbf{q}) = 4J_\parallel \left[ \sin^2\Theta \cos \frac{q_x}{2} \cos \frac{q_y}{2} - \cos^2\Theta \cos(\Phi_{n+1} - \Phi_n) \sin \frac{q_x}{2} \sin \frac{q_y}{2} \right] \quad (7)$$

$$= C_1(\mathbf{q}) + C_2(\mathbf{q}) \cos(\Phi_{n+1} - \Phi_n)$$

$$\gamma_{\phi\phi}^{(n)}(\mathbf{q}) = -4J_\parallel \sin^2\Theta \cos(\Phi_{n+1} - \Phi_n) \sin \frac{q_x}{2} \sin \frac{q_y}{2} \quad (8)$$

$$\gamma_{\theta\phi}^{(n)}(\mathbf{q}) = 4J_\parallel \sin\Theta \cos\Theta \sin(\Phi_{n+1} - \Phi_n) \sin \frac{q_x}{2} \sin \frac{q_y}{2}, \quad (9)$$

where  $C_1 \equiv 4J_\parallel \sin^2\Theta \cos \frac{q_x}{2} \cos \frac{q_y}{2}$  and  $C_2 \equiv -4J_\parallel \cos^2\Theta \sin \frac{q_x}{2} \sin \frac{q_y}{2}$ . Then we expand free energy as  $F = -T \ln Z_0 - T \sum_{k=1}^{\infty} \frac{(-g)^k}{k!} \beta^k \langle V^k \rangle_0^{(c)}$  with  $g$  being a small parameter ( $Z_0 \equiv \text{Tr} e^{-\beta \mathcal{H}_{2D}}$  and  $\langle V^k \rangle_0^{(c)}$  denote the cumulants with respect to  $Z_0^{-1} e^{-\beta \mathcal{H}_{2D}}$ ). To the fourth order in  $g$ , we obtain

$$F = -T \ln Z_0 - \frac{g^2}{2!} A(\Theta) T L^2 \sum_n \cos^2(\Phi_{n+1} - \Phi_n) - \frac{g^4}{4!} B(\Theta) T L^2 \sum_n \cos(\Phi_{n+2} - \Phi_n) - \dots, \quad (10)$$

with the definitions of  $A$  and  $B$  given below. We have dropped several ‘‘biquadratic’’ terms of  $O(g^4)$  because they do not change the  $O(g^2)$  term’s symmetry discussed below.

The  $\{\Phi_n\}$ -dependence of  $F$  lifts part of the ground-state degeneracy, which is unrelated to the system symmetry. The coefficient  $A(\Theta)$  of the  $O(g^2)$  term is determined by the integral

$$\begin{aligned} \beta^2 \langle V^2 \rangle_0^{(c)} &= L^2 \sum_n \int_{\text{BZ}} \frac{d^2 q}{(2\pi)^2} \left[ \frac{\gamma_{\theta\theta}^{(n)}(\mathbf{q})^2}{\omega_\theta(\mathbf{q})^2} + \frac{\gamma_{\phi\phi}^{(n)}(\mathbf{q})^2}{\omega_\phi(\mathbf{q})^2} + 2 \frac{\gamma_{\theta\phi}^{(n)}(\mathbf{q})^2}{\omega_\theta(\mathbf{q})\omega_\phi(\mathbf{q})} \right] \\ &= A(\Theta) L^2 \sum_n \cos^2(\Phi_{n+1} - \Phi_n) + \text{const.} \end{aligned} \quad (11)$$

$A$  is found to be positive, favoring collinear configurations where  $\Phi_{n+1} - \Phi_n = 0$  or  $\pi$ . Therefore, this term represents the biquadratic effective interaction between nearest-neighbor layers. On the other hand, there is no terms proportional to  $\cos(\Phi_{n+1} - \Phi_n)$  in  $F$ , being consistent with the fact that bilinear effective interactions between nearest-neighbor layers are forbidden by the symmetry of the BCT lattice.<sup>10–13)</sup> A mirror-image transformation with respect to the (100) plane that contains (0,0) or (1/2, 1/2) is such a symmetry operation. By the mirror-image transformation with respect to the plane that contains (0,0), for example, sites  $\mathbf{r}$  with  $e^{i\mathbf{Q}\cdot(\mathbf{r}-\mathbf{r}_0^{(n)})} = \pm 1$  in even-numbered (odd-numbered) layers are mapped in sites  $\bar{\mathbf{r}}$  on the same layer with  $e^{i\mathbf{Q}\cdot(\bar{\mathbf{r}}-\mathbf{r}_0^{(n)})} = \pm 1$  ( $e^{i\mathbf{Q}\cdot(\bar{\mathbf{r}}-\mathbf{r}_0^{(n)})} = \mp 1$ ). Consequently, under the corresponding symmetry transformation  $\mathbf{S}_{n,\mathbf{r}} \rightarrow \mathbf{S}'_{n,\mathbf{r}} \equiv \mathbf{S}_{n,\bar{\mathbf{r}}}$ , the local AF moments change as  $e^{i\mathbf{Q}\cdot(\mathbf{r}-\mathbf{r}_0^{(n)})} S_{n,\mathbf{r}}^a \rightarrow e^{i\mathbf{Q}\cdot(\mathbf{r}-\mathbf{r}_0^{(n)})} S_{n,\mathbf{r}}'^a = (-1)^n e^{i\mathbf{Q}\cdot(\bar{\mathbf{r}}-\mathbf{r}_0^{(n)})} S_{n,\bar{\mathbf{r}}}^a$  ( $a = x, y$ ). This means

$\Phi_n \rightarrow \Phi_n$  ( $n$ : even) and  $\Phi_n \rightarrow \Phi_n + \pi$  ( $n$ : odd) for the phase of their spatial average over a layer, resulting in  $\cos(\Phi_{n+1} - \Phi_n)$  being mapped to  $-\cos(\Phi_{n+1} - \Phi_n)$ . Therefore, the two types of the collinear configurations, namely those with AF moments of adjacent layers being parallel ( $\Phi_{n+1} - \Phi_n = 0$ ) or antiparallel ( $|\Phi_{n+1} - \Phi_n| = \pi$ ), are equivalent. While this degeneracy generally exists for the AF moments of any two layers ( $n, n'$ ) with  $|n - n'|$  being an odd number, this is not the case with layers of *even*-numbered separations. Indeed, the  $O(g^4)$  term in  $F$  determined by

$$B(\Theta) \equiv \int_{\text{BZ}} \frac{d^2q}{(2\pi)^2} \frac{48 C_1^2 C_2^2}{\omega_\theta(\mathbf{q})^4} > 0 \quad (12)$$

represents the bilinear effective interaction between second nearest-neighbor layers, favoring  $\Phi_{n+2} - \Phi_n = 0$ .

Although the above spin-wave treatment describes the situation at low temperatures  $T \ll T_c$ , we can expect essentially the same form as eq. (10) also for  $T \lesssim T_c$  in terms of symmetry. Therefore, the ordered phase is expected to have the following characteristics (see Fig. 2). First, there are two subsystems with XY-type 3D ordering, namely even- and odd-numbered layers, but there are no bilinear effective interactions in between. Second, because of the effective biquadratic interactions, the AF moments of these subsystems tend to align in the same direction. As a consequence, there are two symmetrically equivalent but distinct configurations  $\Phi_{n+1} - \Phi_n = 0$  or  $\pi$  (Fig. 2). Note that interlayer bonds that are equivalent by symmetry become inequivalent in the ordered phase, meaning that *bond ordering* results from the spontaneous  $Z_2$  symmetry breaking. These features are qualitatively the same as the original quantum system.<sup>10-13</sup> The bond order is a direct 3D analogue of the ‘‘Ising-order’’ that was discussed in the frustrated square-lattice  $J_1$ - $J_2$  model for  $2J_2 > J_1$ .<sup>18-20</sup> We will use

$$\sigma_{n,\mathbf{r}} = \sum_{\delta\mathbf{r}} \frac{(-1)^{\delta\mathbf{r}}}{4} \left( S_{n,\mathbf{r}}^x S_{n+1,\mathbf{r}+\delta\mathbf{r}}^x + S_{n,\mathbf{r}}^y S_{n+1,\mathbf{r}+\delta\mathbf{r}}^y \right), \quad (-1)^{\delta\mathbf{r}} \equiv \exp[i(\pi, -\pi) \cdot \delta\mathbf{r}] \quad (13)$$

as the local bond-ordering order parameter. It is invariant under  $O(2)$  spin rotations but changes its sign ( $\sigma \rightarrow -\sigma$ ) under mirror-image reflections of the lattice, i.e., it serves to detect the  $Z_2$  symmetry breaking.

### 3. Theoretical Arguments on the Phase Transition

#### 3.1 Single bilayer and the BCT lattice

Let us consider the problem of how many phase transitions take place. There are two possible scenarios: a) only one phase transition at  $T = T_c^{XY} = T_c^{BO}$ , driven by the XY ordering. b) two transitions at  $T = T_c^{BO}$  and  $T = T_c^{XY}$  ( $< T_c^{BO}$ ). Since the XY ordering necessarily accompanies the bond ordering,  $T_c^{XY} > T_c^{BO}$  is impossible. We will use the results of a single *bilayer* case to argue that a) is the correct scenario. The bilayer case is equivalent to the  $J_1$ - $J_2$  XY model with  $J_1 = J_\perp$  and  $J_2 = J_\parallel$ . This model has been studied numerically by Loison and Simon.<sup>20</sup> It breaks the additional  $Z_2$  symmetry for  $2J_2 > J_1$  at a finite temperature

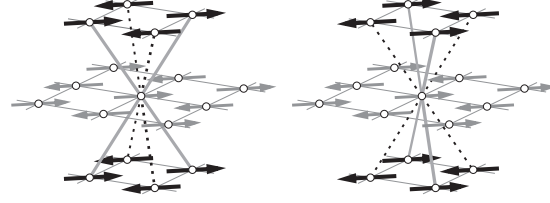


Fig. 2. Expected ordered phase. Solid and gray arrows denote spins on different sublattices, namely, even- and odd-numbered layers, and only their XY components are shown for clarity. These configurations are distinct in the sense of the spontaneous bond ordering (see text). Solid (dashed) interlayer lines represent the spin-pairs with parallel (antiparallel) XY components.

$T = T_c^\kappa$  with a second-order transition, which is followed by a Berezinskii-Kosterlitz-Thouless (BKT)-type transition at a slightly lower temperature  $T = T_{KT} < T_c^\kappa$ .

We next consider an array of weakly coupled bilayers with  $J_f$  being the inter-bilayer interaction ( $J_f/J_\parallel \ll 1$ ), such that the array returns to the original BCT lattice when  $J_f = J_\perp$ . In this case, induced by the order-by-disorder mechanism, there appear effective interlayer interactions  $J'_{eff} = (J_f/J_\parallel)^k J_\parallel$  between the XY-components of spins and effective interlayer interactions  $J''_{eff} = (J_f/J_\parallel)^l J_\parallel$  between bond-ordering order parameters. Equation (10) implies that  $k = 4$ , and also that  $l = 2$  because  $J''_{eff}$  is determined by effective biquadratic interactions. The effective coupling  $J'_{eff}$  is relevant for turning the BKT transition into the true long-range XY ordering and  $J''_{eff}$  drives the 2D bond ordering to the 3D behavior. To determine  $T_c^{XY}$  and  $T_c^{BO}$ , we use a simple random phase approximation (RPA) argument.<sup>21)</sup> In this treatment, the XY and bond orderings take place when

$$J'_{eff} \chi(T_c^{XY}) \approx 1 \quad (14)$$

$$J''_{eff} \chi^\kappa(T_c^{BO}) \approx 1 \quad (15)$$

are satisfied, respectively. Here,  $\chi(T)$  and  $\chi^\kappa(T)$  are the AF XY and 2D bond ordering susceptibilities for the single bilayer, respectively. As the temperature is lowered,  $\chi(T)$  is expected to diverge exponentially as  $\chi(T) \propto J_\parallel^{-1} \exp\left(b\sqrt{\frac{T_{KT}}{T-T_{KT}}}\right)$  with  $b$  being a constant. On the other hand,  $\chi^\kappa(T)$  is expected to show the power-law divergence  $\chi^\kappa(T) \propto J_\parallel^{-1} \left(\frac{T-T_c^\kappa}{T_c^\kappa}\right)^{-\gamma}$  ( $\gamma > 0$ ). By substituting these expressions in eqs. (14) and (15), we obtain:

$$\frac{T_c^{XY} - T_{KT}}{T_{KT}} \approx \left[ \frac{b}{\ln(J'_{eff}/J_\parallel)} \right]^2 = \left[ \frac{b/k}{\ln(J_f/J_\parallel)} \right]^2 \quad (16)$$

$$\frac{T_c^{BO} - T_c^\kappa}{T_c^\kappa} \approx (J''_{eff}/J_\parallel)^{1/\gamma} = (J_f/J_\parallel)^{l/\gamma}. \quad (17)$$

Because eq. (16) diverges as  $J_f$  approaches  $J_\parallel$  while eq. (17) does not, these equations imply that  $T_c^{XY} > T_c^{BO}$  for  $J_f > J_f^c$ . Here,  $J_f^c$  depends on the difference  $T_c^\kappa - T_{KT}$ . Since the difference seems to be very small according to the existing numerical simulations,<sup>22)</sup> we can expect that

$J_f^c$  is small. Therefore, we can conclude that the thermodynamic phase transition of the XY ordering first takes place as temperature decreases over a wide range of  $J_f$  values. Here, note that the above RPA estimate of  $T_c^{BO}$  is based on assumption that the XY spin ordering is absent. Since the XY ordering also breaks the  $Z_2$  symmetry, the bond ordering transition temperature cannot be lower than  $T_c^{XY}$ . Therefore, the above RPA result  $T_c^{XY} > T_c^{BO}$  actually implies a single-phase transition.

### 3.2 Stability of the decoupled XY fixed point

The next question is about the universality class of the phase transition, in particular as to whether it belongs to the previously expected 3D XY universality class. Introducing the “continuous”  $O(2)$  real vectors  $\phi_i^a(r)$  ( $a = x, y$ ) to describe the spins on the even- ( $i = 1$ ) and odd-numbered ( $i = 2$ ) layers,<sup>23)</sup> we consider the Landau-Ginzburg-Wilson (LGW)-type effective Hamiltonian of the form

$$\mathcal{H}_{eff} = \int \left[ \frac{1}{2} \sum_{\mu} (\partial_{\mu} \phi_1 \cdot \partial_{\mu} \phi_1 + \partial_{\mu} \phi_2 \cdot \partial_{\mu} \phi_2) + t (|\phi_1|^2 + |\phi_2|^2) + u (|\phi_1|^4 + |\phi_2|^4) + \lambda (\phi_1 \cdot \phi_2)^2 + g |\phi_1|^2 |\phi_2|^2 \right] d^d r. \quad (18)$$

The first three terms constitute a standard  $\phi^4$  theory for the decoupled  $O(2)$  model. The  $(\phi_1 \cdot \phi_2)^2$  term represents a quadrupole-quadrupole interaction induced by the order-by-disorder mechanism. The other quartic term  $|\phi_1|^2 |\phi_2|^2$  is included here explicitly, because it is generated through renormalization group (RG) iterations. As we mentioned earlier, the lattice-symmetry of the original model eq. (1) does not allow effective bilinear interactions between nearest-neighbor layers. For this reason, the quadratic term  $\phi_1 \cdot \phi_2$  is impossible in eq. (18).

This Hamiltonian eq. (18) is an  $N = M = 2$  case of the model referred to as the “ $N$ -coupled  $M$ -vector model,”<sup>24)</sup> with the additional  $(\phi_1 \cdot \phi_2)^2$  term. It has a trivial *decoupled fixed point* (D) at  $u \neq 0$  and  $\lambda = g = 0$ , which is a plausible candidate for the fixed point corresponding to the expected 3D XY universality. This model was first introduced in the 1970s,<sup>25)</sup> in the context of the replica theory for random systems. It was found that the decoupled fixed point is *unstable* against perturbations such as biquadratic ones. Below, we briefly summarize the argument, because the original argument was made in a relatively different context.

The stability of a fixed point against a given perturbation is determined by the RG of its conjugate field. Therefore, we need to compute the RG eigenvalues  $y_{\lambda, D}$  ( $y_{g, D}$ ) of the coupling  $\lambda$  ( $g$ ) at the decoupled fixed point. They can be computed via two-point correlators at the decoupled fixed point, which in this case can be readily factorized into known correlators. First,

$$\langle |\phi_1(r)|^2 |\phi_2(r)|^2 |\phi_1(r')|^2 |\phi_2(r')|^2 \rangle_D = \langle |\phi_1(r)|^2 |\phi_1(r')|^2 \rangle_D \langle |\phi_2(r)|^2 |\phi_2(r')|^2 \rangle_D$$

$$\propto |r - r'|^{-4x_t}, \quad (19)$$

where  $x_t = d - 1/\nu$  is the scaling dimension of the energy-density field of the 3D XY model with  $\nu$  being the correlation-length exponent. This means that the scaling dimension of the  $|\phi_1|^2|\phi_2|^2$  term is equal to  $2x_t$ . Therefore,

$$y_{g,D} = d - 2x_t = 2/\nu - d \approx -0.021815 < 0 \text{ in } d = 3, \quad (20)$$

where we used  $\nu = 0.67155(27)$ .<sup>26)</sup> The negative  $y_{g,D}$  indicates that the decoupled fixed point is stable against the  $|\phi_1|^2|\phi_2|^2$  term. However, this is not the case with the other  $(\phi_1 \cdot \phi_2)^2$  term. This term can be decomposed into

$$(\phi_1 \cdot \phi_2)^2 = \frac{1}{2} (Q_1^{xx} Q_2^{xx} + Q_1^{xy} Q_2^{xy} + |\phi_1|^2 |\phi_2|^2), \quad (21)$$

where  $Q_i^{xx} = (\phi_i^x)^2 - (\phi_i^y)^2$  and  $Q_i^{xy} = 2\phi_i^x \phi_i^y$  ( $i = 1, 2$ ) are components of the traceless symmetric tensor of the quadrupole order parameter. Using eq. (21) and the O(2) invariance of  $\mathcal{H}_{eff}$ , we obtain

$$\begin{aligned} & 4 \langle (\phi_1 \cdot \phi_2)^2(r) (\phi_1 \cdot \phi_2)^2(r') \rangle_D \\ &= 2 \langle Q_1^{xx}(r) Q_1^{xx}(r') \rangle_D \langle Q_2^{xx}(r) Q_2^{xx}(r') \rangle_D + \langle \phi_1^2(r) \phi_1^2(r') \rangle_D \langle \phi_2^2(r) \phi_2^2(r') \rangle_D \\ &= \frac{C_{QQ}}{|r - r'|^{4x_Q}} + \frac{C_{tt}}{|r - r'|^{4x_t}}, \quad (22) \end{aligned}$$

where  $C_{QQ}$  and  $C_{tt}$  are nonzero coefficients and  $x_Q$  is the scaling dimension of the quadrupole order parameter. Comparing  $x_Q \approx 1.237^{27)}$  with  $x_t \approx 1.5109$ ,<sup>26)</sup> we find that the quadrupole-quadrupole correlator gives the most relevant contribution to eq. (22). Consequently, the scaling dimension of the  $(\phi_1 \cdot \phi_2)^2$  term is equal to  $2x_Q$  and we obtain

$$y_{\lambda,D} = d - 2x_Q \approx 0.526. \quad (23)$$

The positive  $y_{\lambda,D}$  indicates that  $\lambda$  is a relevant coupling for the decoupled 3D XY fixed point. In other words, the decoupled fixed point is unstable under such perturbation.

#### 4. Results of the Monte Carlo Simulation

In this section, we present the results our Monte Carlo (MC) simulation for the Hamiltonian eq. (1). All the results shown in what follows are obtained for  $J_{\perp}/J_{\parallel} = 0.75$  and  $H/J_{\parallel} = 10.0$ . The system size is  $L \times L \times (L/4)$  with  $L = 16, 24, 32, 40$ , and 48. Our main motivation for these parameters and the anisotropic aspect ratio is to realize the proper configuration in finite-size systems. These considerations are necessary, because fluctuation-induced effective couplings, if normalized per site, are typically smaller than  $J_{\parallel}$  by 2–3 orders of magnitude.

Figures 3 and 4 show low-temperature snapshots of MC simulations, which are useful for understanding the situation. The points in these figures represent the local XY AF moments

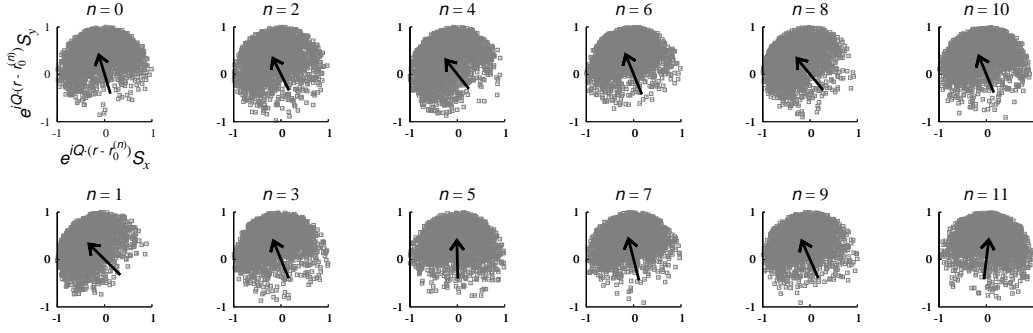


Fig. 3. Low-temperature snapshot of a MC simulation for  $L = 48$  at  $T/J_{\parallel} = 0.27$  (see text).

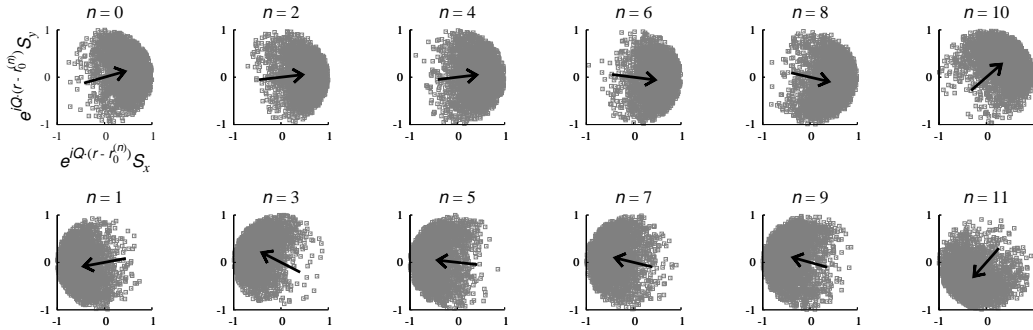


Fig. 4. Snapshot under the same conditions as the snapshot in Fig. 3, but obtained using a different random-number sequence.

$e^{i\mathbf{Q}\cdot(\mathbf{r}-\mathbf{r}_0^{(n)})}(S_n^x, S_n^y)$  in each layer, with their spatial positions being discarded for clarity; the arrows represent the in-layer AF moments. We can see that the configurations are collinear, and that the AF-moments in every other layer tend to align in the same direction. By comparing these two figures, we can also see that the effective interaction between layers of odd-number separations is not bilinear but biquadratic. As we will quantitatively show below, these configurations are typical at low temperatures.

In Figs. 5(a) and 5(b), we show decays of the correlation function  $G(\mathbf{R}) \equiv G(\mathbf{R}(n, \mathbf{r}; n', \mathbf{r}')) = \langle S_{n,\mathbf{r}}^x S_{n',\mathbf{r}'}^x + S_{n,\mathbf{r}}^y S_{n',\mathbf{r}'}^y \rangle$  along the interlayer [111] and intralayer [110] directions.  $G(\mathbf{R})$  along [110] indicates the formation of the in-layer AF order, and positive correlations along [111] for  $\mathbf{R}/(1/2, 1/2, 1/2) = 2$  and 4 suggest the presence of a bilinear effective interlayer interaction of the ferromagnetic type. On the other hand, the suppression of  $G(\mathbf{R})$  for  $\mathbf{R}/(1/2, 1/2, 1/2) = 1$  and 3 is mainly due to the cancellation of the contributions of opposite (“parallel” and “antiparallel”) configurations, suggesting the absence of a bilinear effective interaction between nearest-neighbor layers; nonzero values at these distances are

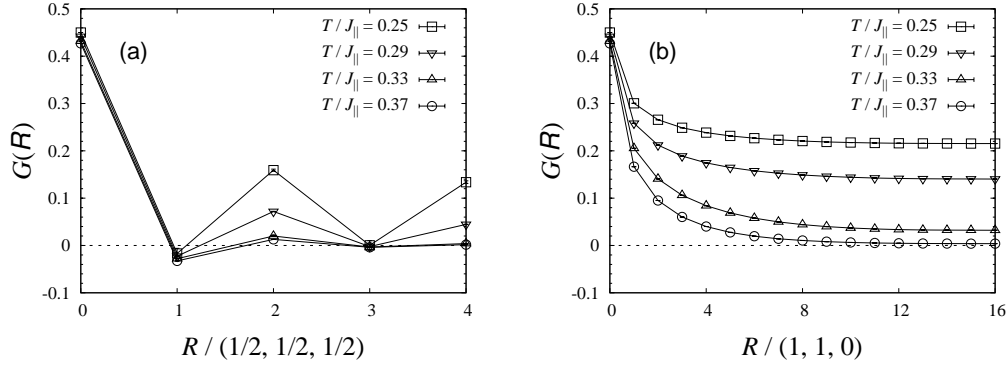


Fig. 5. Correlation function  $G(\mathbf{R})$  along [111] (a) and [110] (b) for  $L = 32$ . The lines are guides to the eyes.

due to short-wavelength fluctuations.

Next we turn to the analysis of the order parameters. There are two relevant order parameters to be examined: the XY and bond-ordering order parameters. We use

$$\mathbf{M}_{XY} \equiv \frac{8}{L^3} \sum_{n \in \text{even}, \mathbf{r}} e^{i\mathbf{Q} \cdot (\mathbf{r} - \mathbf{r}_0^{(n)})} (S_{n,\mathbf{r}}^x \hat{\mathbf{x}} + S_{n,\mathbf{r}}^y \hat{\mathbf{y}}), \quad (24)$$

as the XY order parameter, namely, an AF order parameter defined on the “even” sublattice (the choice of either “even” or “odd” is arbitrary). On the other hand, we use  $M_{BO} \equiv \frac{4}{L^3} \sum_{n,\mathbf{r}} \sigma_{n,\mathbf{r}}$  as the bond-ordering order parameter ( $\sigma_{n,\mathbf{r}}$  is defined by eq. (13)).

Figures 6(a) and 6(b) show the temperature dependence of the Binder parameters  $U_4^{XY} \equiv \langle \mathbf{M}_{XY}^4 \rangle / \langle \mathbf{M}_{XY}^2 \rangle^2$  and  $U_4^{BO} \equiv \langle M_{BO}^4 \rangle / \langle M_{BO}^2 \rangle^2$ . They should asymptotically show crossings for different system sizes at critical points, whereas  $U_4^{XY} \rightarrow 2$  and  $U_4^{BO} \rightarrow 3$  for  $T/J_{\parallel} \gg 1$ , and  $U_4^{XY}, U_4^{BO} \rightarrow 1$  for  $T/J_{\parallel} \ll 1$ . It is not easy to determine  $T_c^{XY}$  and  $T_c^{BO}$  precisely as they still suffer from severe finite-size effects, but it is clear that there is a phase transition. Both  $T_c^{XY}$  and  $T_c^{BO}$  are located in the region  $0.305 < T/J_{\parallel} < 0.310$ .

In order to obtain the critical exponents, we perform finite-size scaling analysis of the squared quantities  $\langle \mathbf{M}_{XY}^2 \rangle$  and  $\langle M_{BO}^2 \rangle$  assuming the following standard scaling forms:

$$\langle \mathbf{M}_{XY}^2 \rangle = L^{-(d-2+\eta)} \Phi_{XY}(tL^{1/\nu}), \quad (25)$$

$$\langle M_{BO}^2 \rangle = L^{-2x_{\sigma}} \Phi_{BO}(t'L^{1/\nu'}), \quad (26)$$

where  $t \equiv (T - T_c^{XY})/T_c^{XY}$  and  $t' \equiv (T - T_c^{BO})/T_c^{BO}$  are reduced temperatures,  $\Phi_{XY}$  and  $\Phi_{BO}$  are scaling functions,  $x_{\sigma}$  is the scaling dimension of the bond order parameter, and the exponents  $\nu$ ,  $\nu'$ , and  $\eta$  are conventional parameters. As shown in Figs. 7(a) and 7(b), we can produce a reasonable data collapse, where we use

$$\eta = 0.04(1), \quad \nu = 0.67(1), \quad \text{and} \quad T_c^{XY}/J_{\parallel} = 0.308(1) \quad (27)$$

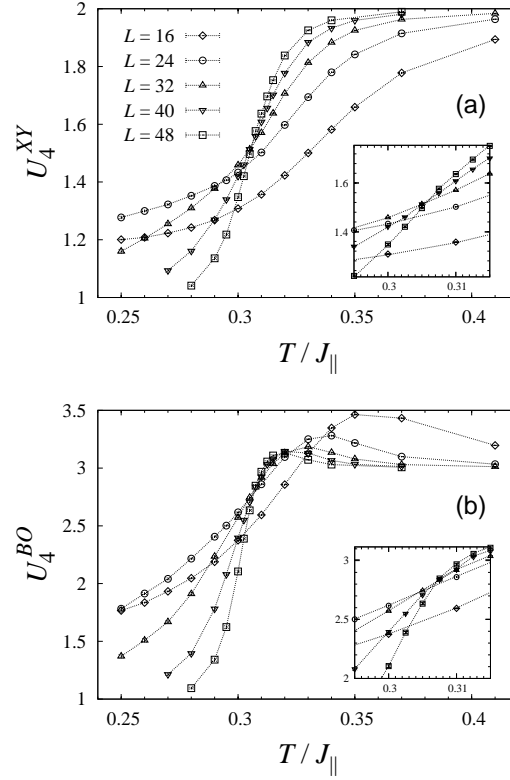


Fig. 6. Temperature dependence of the Binder parameters of the (a) XY ordering and (b) bond ordering. The insets show enlarged views in the critical region. The lines are guides to the eyes.

for the XY ordering and

$$2x_\sigma = 2.07(1), \quad \nu' = 0.67(1), \quad \text{and} \quad T_c^{BO}/J_{||} = 0.310(2) \quad (28)$$

for the bond ordering. These values of  $T_c^{XY}$  and  $T_c^{BO}$  are consistent with the estimations made from the Binder parameters.

Although there is a slight difference between  $T_c^{XY}$  and  $T_c^{BO}$ , the close proximity of  $\nu$  and  $\nu'$  (no difference in our resolution) suggests that the difference found for  $L \leq 48$  is due to finite-size effects and that there is only one transition. As for the critical exponents, their values agree with those of the decoupled 3D XY fixed point, for which  $\eta_D$  and  $\nu_D$  coincide with those of the 3D XY model ( $\eta = 0.0380(4)$  and  $\nu = 0.67155(27)^{26}$ ) and, in addition,  $x_{\sigma,D} = 2x$  holds with  $x$  being the scaling dimension of the XY order parameter (therefore,  $2x_{\sigma,D} = 2 \cdot 2x = 2(d - 2 + \eta) = 2.0760(8)$ ).<sup>13)</sup> The reason for this is that  $\sigma$  corresponds to  $\phi_1 \cdot \phi_2$  in the continuous-spin language. Its two-point correlator can be factorized as

$$\langle (\phi_1 \cdot \phi_2)(r) (\phi_1 \cdot \phi_2)(r') \rangle_D = \langle \phi_1(r) \cdot \phi_1(r') \rangle_D \langle \phi_2(r) \cdot \phi_2(r') \rangle_D \quad (29)$$

using the O(2) symmetry of the Hamiltonian eq. (1) or (18). Then, the simple counting of powers leads to  $x_{\sigma,D} = 2x$ .

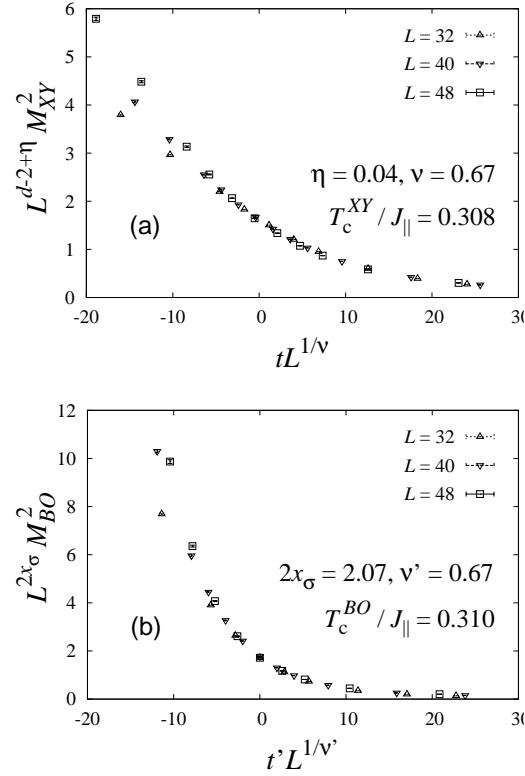


Fig. 7. Finite-size scaling plots of (a)  $\langle M_{XY}^2 \rangle$  and (b)  $\langle M_{BO}^2 \rangle$ .

## 5. Discussion

The MC results apparently contradict the previous observation that the decoupled fixed point is unstable, but the reason why critical exponents of such an unstable fixed point are obtained can be understood through the theory of crossover behavior. First, the above MC results suggest that the actual RG flow passes through the vicinity of the decoupled fixed point. In this parameter region, the system-size dependence of the singular part of free energy has the scaling form

$$f_s(t, \lambda, L) = |t|^{d\nu_D} \Psi \left( tL^{1/\nu_D}, \lambda L^{y_{\lambda,D}} \right). \quad (30)$$

The amplitude of the relevant biquadratic coupling  $\lambda$  can be estimated as  $|\lambda| \sim (J_{\perp}/J_{\parallel})^2 A \approx 0.022$  using eq. (10). It is too small to observe any significant sign of the crossover behavior in the sense that we need a system as large as  $L \sim |\lambda|^{-1/y_{\lambda,D}} \approx 1400$ , which is much larger than the largest system investigated in the present work. In this way, the most natural interpretation of our MC results is summarized as follows: what we obtained are “effective” exponents due to transient behavior of the RG flow around the decoupled fixed point. However, since the flow should eventually leave the vicinity of the decoupled fixed point, we expect a crossover to be observed in larger systems.

The above finite-size scaling arguments can be immediately translated into general scaling

arguments, in which experimental relevance becomes more transparent. The fact that the RG flow passes through the vicinity of the decoupled fixed point means that there is a certain temperature region where long-wavelength fluctuations are described by the decoupled 3D XY model. However, because this fixed point is unstable, this temperature region must be outside of the ultimate critical region:  $|t| \gtrsim t_X$  such that the correlation length is bounded as  $\xi \lesssim |\lambda|^{-1/y_{\lambda,D}}$ .<sup>28)</sup> We expect that, as one approaches the critical point beyond this intermediate temperature region, a crossover from the decoupled 3D XY behavior appears.

A question that now arises concerns the nature of the stable fixed point. Since the perturbation field  $\lambda$  is only slightly relevant at the decoupled fixed point for  $d$  sufficiently close to 4 ( $y_{\lambda,D} = \frac{3}{5}\epsilon + O(\epsilon^2)$  with  $\epsilon \equiv 4 - d$ ), it does not seem to be difficult to find a new stable fixed point by performing the  $\epsilon$ -expansion in the lowest nontrivial order. However, the attempt to conduct  $O(\epsilon)$  calculation is unsatisfactory.<sup>25)</sup> According to such a calculation, there is no stable fixed point in the finite region of the parameter space. Moreover, it fails to reproduce the irrelevance of  $g$  around the decoupled fixed point, implying that the topology of the flow itself may not be convincing unless one goes to sufficiently high orders in  $\epsilon$ . Therefore, it remains to be clarified whether a stable fixed point exists and, if it does, what type of critical behavior is expected from such a fixed point. We expect that direct numerical simulations of the effective Hamiltonian eq. (18) will shed light on this problem. Such a simulation will be performed in a future study.

## 6. Conclusions

In this paper, we have studied a classical model of the finite-temperature transition in BaCuSi<sub>2</sub>O<sub>6</sub>. We have demonstrated that thermal fluctuations select a particular configuration in a low-temperature ordered phase. It is stabilized by a composite of two subsystems, and is realized via multiple symmetry breakings, O(2) and Z<sub>2</sub>, with the latter being related to the mirror-image reflection symmetry of the underlying lattice. The qualitative characteristics of the phase are the same as those of the original quantum system. On the basis of the RPA argument, we have also argued that there is only one transition at which the XY and bond orderings occur simultaneously in contrast to the 2D single-bilayer case. As for the critical behavior of the phase transition, we have shown that a plausible form of LGW-type effective Hamiltonian has a decoupled fixed point that yields the critical exponents of the 3D XY universality class. However, scaling arguments reveal that the decoupled fixed point is unstable against the perturbation of the quadrupole-quadrupole interaction. Since the quadrupole-quadrupole interaction is induced by the order-by-disorder effect, this conclusion clearly excludes the decoupled XY fixed point for describing the asymptotic critical behavior. On the other hand, MC simulation yields a set of exponents that can be attributed to the decoupled 3D XY universality. As a first point to be noticed from this observation, we have indicated that there is actually an intermediate temperature region outside the ultimate

critical region, where the observed thermodynamic properties are related to the decoupled fixed point. We have also presented a reasonable argument explaining why no significant deviation has been observed (within our system sizes) from the critical exponents of the unstable decoupled fixed point, on the basis of the theory of crossover behavior.

### **Acknowledgments**

We thank H. Tsunetsugu, M. Oshikawa, and D. Uzunov for valuable discussions. We also thank T. Suzuki for his critical reading of the manuscript. The computation in the present work is executed on computers at the Supercomputer Center, Institute for Solid State Physics, University of Tokyo. The present work is financially supported by the MEXT Global COE Program “the Physical Science Frontier,” the MEXT Grand-in-Aid for Scientific Research (B) (19340109), the MEXT Grand-in-Aid for Scientific Research on Priority Areas “Novel States of Matter Induced by Frustration” (19052004), and the Next Generation Supercomputing Project, Nanoscience Program, MEXT, Japan.

## References

- 1) See, for example, T. Giamarchi, C. Rüegg, and O. Tchernyshyov: *Nature Phys.* **4** (2008) 198.
- 2) S. E. Sebastian, N. Harrison, C. D. Batista, L. Balicas, M. Jaime, P. A. Sharma, N. Kawashima, and I. R. Fisher: *Nature (London)* **441** (2006) 617.
- 3) Y. Sasago, K. Uchinokura, A. Zheludev, and G. Shirane: *Phys. Rev. B* **55** (1997) 8357.
- 4) M. Jaime, V. F. Correa, N. Harrison, C. D. Batista, N. Kawashima, Y. Kazuma, G. A. Jorge, R. Stern, I. Heinmaa, S. A. Zvyagin, Y. Sasago, and K. Uchinokura: *Phys. Rev. Lett.* **93** (2004) 087203.
- 5) K. M. Sparta and G. Roth: *Acta Crystallogr., Sect. B* **60** (2004) 491.
- 6) S. E. Sebastian, P. A. Sharma, M. Jaime, N. Harrison, V. Correa, L. Balicas, N. Kawashima, C. D. Batista, and I. R. Fisher: *Phys. Rev. B* **72** (2005) 100404(R).
- 7) E. C. Samulon, Z. Islam, S. E. Sebastian, P. B. Brooks, M. K. McCourt, Jr., J. Ilavsky, and I. R. Fisher: *Phys. Rev. B* **73** (2006) 100407(R).
- 8) C. Rüegg, D. F. McMorrow, B. Normand, H. M. Rønnow, S. E. Sebastian, I. R. Fisher, C. D. Batista, S. N. Gvasaliya, C. Niedermayer, and J. Stahn: *Phys. Rev. Lett.* **98** (2007) 017202.
- 9) S. Krämer, R. Stern, M. Horvatić, C. Berthier, T. Kimura, and I. R. Fisher: *Phys. Rev. B* **76** (2007) 100406(R).
- 10) O. Rösch and M. Vojta: *Phys. Rev. B* **76** (2007) 180401(R).
- 11) O. Rösch and M. Vojta: *Phys. Rev. B* **76** (2007) 224408.
- 12) C. D. Batista, J. Schmalian, N. Kawashima, P. Sengupta, S. E. Sebastian, N. Harrison, M. Jaime, and I. R. Fisher: *Phys. Rev. Lett.* **98** (2007) 257201.
- 13) J. Schmalian and C. D. Batista: *Phys. Rev. B* **77** (2008) 094406.
- 14) N. Laflorencie and F. Mila: *Phys. Rev. Lett.* **102** (2009) 060602.
- 15) Inhomogeneity is known to exist in the intradimer interaction on different layers, and several authors argued that the 2D-like power law can be explained by this inhomogeneity.<sup>11, 14)</sup> However, to concentrate on the role of the frustration, we do not take it into account.
- 16) T. Giamarchi and A. M. Tsvelik: *Phys. Rev. B* **59** (1999) 11398.
- 17) J. Villain, R. Bidaux, J. P. Carton, and R. Conte: *J. Phys. (Paris)* **41** (1980) 1263.
- 18) C. Henley: *Phys. Rev. Lett.* **62** (1989) 2056.
- 19) P. Chandra, P. Coleman, and A. I. Larkin: *Phys. Rev. Lett.* **64** (1990) 88.
- 20) D. Loison and P. Simon: *Phys. Rev. B* **61** (2000) 6114.
- 21) W. Janke and T. Matsui: *Phys. Rev. B* **42** (1990) 10673.
- 22) To be explicit,  $T_{KT}/J_1 = 0.56271(5)$  and  $T_c^*/J_1 = 0.56465(8)$  for  $J_2/J_1 = 0.7^{20)}$
- 23) There should be no confusion with the phase of the local AF moment.
- 24) A. Aharony: in *Phase Transitions and Critical Phenomena*, ed. C. Domb and M. S. Green (Academic Press, London, 1976) Vol. 6, p. 357.
- 25) A. Aharony: *Phys. Rev. B* **12** (1975) 1038.
- 26) M. Campostrini, M. Hasenbusch, A. Pelissetto, P. Rossi, and E. Vicari: *Phys. Rev. B* **63** (2001) 214503.
- 27) P. Calabrese and P. Parruccini: *Phys. Rev. B* **71** (2005) 064416.
- 28) Even though the finite-temperature transition can be essentially described by the classical theory, quantum effects must be taken into account for the quantitative estimate of  $\lambda$  (and  $t_X$ ) for real

systems such as  $\text{BaCuSi}_2\text{O}_6$ .